PCCP

RSC Publishing

PAPER

Li diffusion through doped and defected graphene†

Deya Das,[a] Seungchul Kim,[b] Kwang-Ryeol Lee[b] and Abhishek K. Singh*[a]

Cite this: *Phys. Chem. Chem. Phys.*, 2013, **15**, 15128

Received 12th July 2013,
Accepted 17th July 2013

DOI: 10.1039/c3cp52891j

www.rsc.org/pccp

We investigate the effect of nitrogen and boron doping on Li diffusion through defected graphene using first principles based density functional theory. While a high energy barrier rules out the possibility of Li- diffusion through the pristine graphene, the barrier reduces with the incorporation of defects. Among the most common defects in pristine graphene, Li diffusion through the divacancy encounters the lowest energy barrier of 1.34 eV. The effect of nitrogen and boron doping on the Li diffusion through doped defected-graphene sheets has been studied. N-doping in graphene with a monovacancy reduces the energy barrier significantly. The barrier reduces with the increasing number of N atoms. On the other hand, for N doped graphene with a divacancy, Li binds in the plane of the sheet, with an enhanced binding energy. The B doping in graphene with a monovacancy leads to the enhancement of the barrier. However, in the case of B-doped graphene with a divacancy, the barrier reduces to 1.54 eV, which could lead to good kinetics. The barriers do not change significantly with B concentration. Therefore, divacancy, B and N doped defected graphene has emerged as a better alternative to pristine graphene as an anode material for Li ion battery.

1 Introduction

Li ion batteries (LIB) are the most promising energy storage devices for today's technologies due to their size, portability, and superior performance.[1–6] Recent progress in the miniaturization of electronic devices and the advent of hybrid electric vehicles have set a demand for LIBs with anode materials having specific capacity far beyond that of the existing commercially used graphite (372 mA h g^{-1}).[7,8] Together with high capacity, a promising anode material should also possess a low operating potential, a low barrier for Li intercalation and a high interfacial stability. Due to its high theoretical specific capacity[9,10] of approximately 4200 mA h g^{-1} for $Li_{22}Si_5$, silicon has become the most attractive anode material to replace graphite. However, silicon-based anode materials face poor electrochemical performances[11] caused by enormous volume changes due to lithiation–delithiation. Further challenges arise from the continuous formation of a solid electrolyte interface (SEI), which results in poor interfacial properties.

In order to protect the silicon anode, carbon based nanomaterials such as graphene[12] and fullerene[13] have been investigated as a coating, which acts as an artificial solid electrolyte interface. Experimentally, Wang *et al.*[12] developed silicon based anodes overlapped by adaptable graphene sheets to prevent the direct exposure to the electrolyte. These silicon–carbon nanocables are sandwiched between reduced graphene oxide sheets to solve the problem of volume change, while at the same time maintaining the structural and electrical integrity of the anode. In this case, a high reversible specific capacity of 1600 mA h g^{-1} at 2.1 A g^{-1} has been reported.

Besides an artificial SEI, graphene emerges as a strong candidate for anode materials[14–16] in Li ion batteries due to its high surface area, high electrical conductivity and robust mechanical integrity. It shows a higher capacity of about 540 mA h g^{-1} compared to the graphite anode.[17] Moreover, due to the reduced dimensions of graphene, in an electrochemical cell, current rates can be enhanced as the diffusion time of Li ions (t) is directly proportional to the square of the diffusion length (L), $t = L^2/D$, where D is the diffusion coefficient.[18] The success of both of the applications of graphene, namely, an anode material or artificial SEI, depends strongly on the rate of diffusion of Li, through and along the graphene sheet.

Here, we study the Li diffusion through the graphene sheet using first principles calculations. For pristine graphene, the energy barrier is very high. In order to reduce the energy barrier, we investigated Li diffusion through graphene with the most commonly observed defects. The energy barrier has been calculated in the case of undoped defected graphene, including vacancies and the Stone–Wales defect. The barriers are reduced significantly by the presence of defects, with the incorporation of a divacancy having the lowest barrier. We explore doping as another alternative to manipulate Li

[a] *Materials Research Centre, Indian Institute of Science, Bangalore 560012, India. E-mail: abhishek@mrc.iisc.ernet.in*

[b] *Korea Institute of Science and Technology, Hwarangno 14-gil 5, Seongbuk-gu, Seoul 136-791, Korea*

† Electronic supplementary information (ESI) available. See DOI: 10.1039/c3cp52891j

diffusion rate. We studied the effect of both boron and nitrogen doping by calculating the energy barrier through the defected doped graphene sheets. The height of the barrier depends sensitively on the concentration and type of dopants. While, for graphene with a divacancy, nitrogen doping leads to strong binding, boron doped defected graphene show consistently low barriers. Divacancy and a boron doped divacancy emerge as the best candidates for anode materials.

2 Methodology

The first principles calculations were performed using density functional theory (DFT) as implemented in the Vienna *ab initio* simulation package (VASP).[19,20] Electron–ion interactions were described using all-electron projector augmented wave (PAW) pseudopotentials.[21] Electronic exchange and correlation were approximated by a Perdew–Burke–Ernzerhof generalized gradient approximation.[22,23] The periodic images are separated by a 15 Å vacuum along three directions. For all the calculations, the Brillouin zone is sampled by a Gamma point. A conjugate gradient scheme is used to relax the structures until the component of the forces on each atom was ≤ 0.005 eV Å^{-1}. The cutoff energy was set to 400 eV to ensure the accuracy of the results.

3 Results and discussion

In order to compare binding strength of Li in graphene based systems, the adsorption energy (E_{ad}) has been calculated by using the following equation

$$E_{ad} = E_{Sy+Li} - E_{Sy} - E_{Li}$$

where E_{Sy+Li}, E_{Sy} and E_{Li} are the total energies of system with Li, system and bulk Li, respectively. E_{Li} has been calculated considering the Li bulk structure having a body centered cubic (bcc) structure. A graphene sheet has been modeled by a cluster having 54 carbon atoms with the edge passivated by 18 hydrogen atoms (Fig. 1(a)). A cluster structure is more appropriate to describe the effect of the localized defect in the system compared to the periodic model. In the periodic model, the long range elastic forces in the solid can diverge the energy due to the spurious interaction among the defects present in the system and its periodic images.[24] This problem can be avoided in the cluster model where the stresses can be completely relaxed.

The Li adsorption energies on graphene have been calculated by optimizing the structures with three symmetrically non-equivalent sites for Li; (i) bridge (A), (ii) top (B) and (iii) center (C) of the hexagon as shown in the Fig. 1(b) inset. Li is kept initially at a distance of 1.95 Å above the plane of the graphene sheet. In all the three cases, after relaxation Li goes above the center of the hexagon (C) at the distance of 1.72 Å away from the plane of the sheet. The adsorption energy is given in Table 2. The positive adsorption energy of Li for the pristine graphene sheet denotes that Li-graphene binding is not so strong and therefore, there will be finite chance of clustering of the Li atoms. This would hinder the diffusion of Li.

Next, we calculate the energy barrier for Li to diffuse through the graphene plane. In order to save computational time, the barriers were calculated without relaxing the intermediate structures. This turns out to be a good approximation as relaxation plays a very small role in bringing down the barrier height. We validate our approach for a few representative systems against a computationally expensive nudged elastic band (NEB) method.[25,26] The barrier height obtained by using both methods are in close agreement (0.5–10% range), as shown in the Table 1. The corresponding plots for the comparison of both methods were discussed in Fig. S1 (ESI†). The equilibrium structure of Li adsorbed on a graphene sheet at the centre of the hexagon is taken as the initial stage for Li to diffuse through. The barrier for the Li diffusion through the graphene sheet is found to be 10.02 eV, as shown in Fig. 1(b). The barrier is in good agreement with the reported value.[27] However, the barrier is very high and for all practical purposes the diffusion through the graphene sheets at the ambient condition will not be possible.

We explore the possibility of Li diffusion through the graphene with a vacancy. Experimentally, it has been shown[28] that enhanced power delivery and excellent high-rate lithium storage capabilities can be achieved by introducing in-plane porosity into the graphene paper electrodes. As expected, the energy barriers through monovacancy (8.18 eV) and divacancy (1.34 eV) graphene are significantly lower than the pristine graphene as shown in Fig. 2. Although the barrier is prohibitively large for the monovacancy, for the divacancy, it is much lower and lies within the range to obtain faster Li kinetics

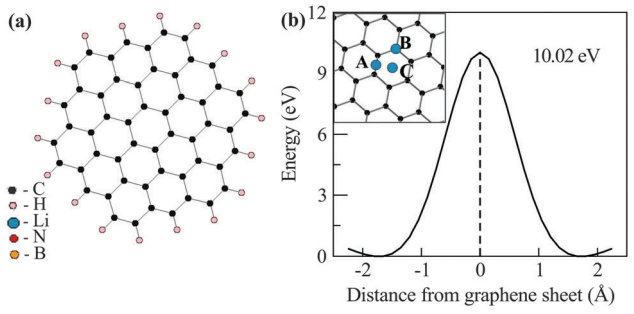

Fig. 1 (a) Cluster of graphene with 54 carbon atoms passivated by 18 hydrogen atoms at the edges and (b) energy barrier for Li diffusion through the pristine graphene sheet *via* the center of the hexagon. Inset: three initial positions of Li marked as A, B, and C, all of them relax back to C.

Table 1 Comparison of energy barriers (E_b) obtained by a single point (SP) calculation and nudged elastic band (NEB) method for a few representative systems

System	E_b by SP (eV)	E_b by NEB (eV)	Error (%)
Pristine graphene	10.02	10.07	0.49
Gr-di	1.34	1.43	6.29
Gr-mono-3N	1.77	1.96	9.69
Gr-di-2B (type 2)	1.54	1.68	8.33

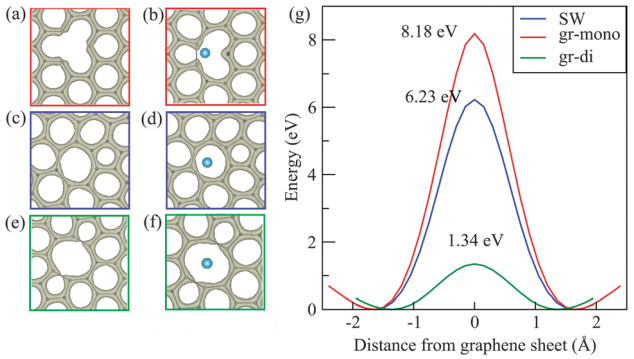

Fig. 2 Isosurfaces of the total electronic charge density of undoped graphene: for monovacancy (a) without and (b) with Li, for Stone Wales defect (c) without and (d) with Li, for divacancy (e) without and (f) with Li, and (g) corresponding energy barriers.

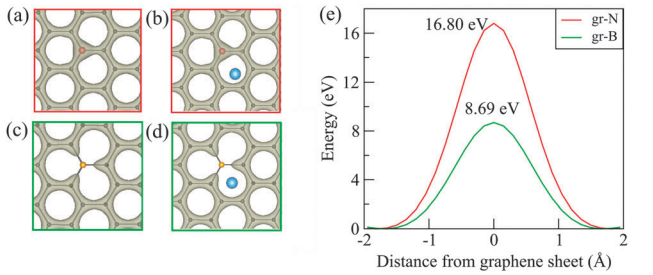

Fig. 3 Isosurfaces of total electronic charge density for pristine graphene: doped by N (a) without and (b) with Li, doped by B (c) without and (d) with Li, and (e) corresponding energy barriers.

under the typical charging conditions of the battery. In the case of the divacancy, the relaxed graphene structure leads to the formation of an octagon surrounded by two pentagons and hexagons as shown in the Fig. 2(e). This large open space helps Li to diffuse quickly.

We considered another common defect in pristine graphene, namely the Stone–Wales defect (SW) where due to the rotation of one C–C bond by 90° with respect to the midpoint of the bond, the six-membered rings of graphene rearrange into a pentagon–heptagon pair.[29,30] Li diffusion has been investigated through the heptagon of the SW defect. The barrier for this system is 6.23 eV, lying between that of monovacancy and divacancy, as shown in Fig. 2. The reduced barrier is caused by the strain induced by formation of the SW defect. We also calculated the adsorption energies of Li on undoped defected graphene. The adsorption energies for monovacancy, divacancy, and SW are −2.03 eV, −0.55 eV and −0.65 eV, respectively. All of the adsorption energies are negative and hence thermodynamically they all should avoid the clustering of Li. The relatively strong binding energy of Li to the monovacancy originates from the formation of a pentagon caused by the presence of a radical as shown in the Fig. 2(b). Since both the SW and the divacancy have no such unsaturated radicals, Li adsorption energies are therefore moderate. These indeed are good propositions as the system will avoid the clustering of Li without affecting the kinetics.

Next, we study the effect of doping on the Li diffusion barrier through the defected graphene. Recent progress in the doping of graphene[31–35] and carbon nanotubes[36–39] with N and B, has brought additional functionality to these wonder materials. Experimentally, N and B doped graphene sheets are investigated for Li ion batteries by calculating capacity, coulomb efficiency and cyclability. Wu *et al.*[31] reported experimentally a very high capacity of 199 and 235 mA h g^{-1} obtained for the N- and B-doped graphene respectively at 25 A g^{-1} (about 30 seconds to full charge). Also, N and B doping have been studied theoretically in the defected graphene for the purpose of lithium storage by calculating the specific capacity.[40,41] These studies, however, do not show the effect of N or B doping on the diffusion barrier of Li. This is important to establish the candidacy of these materials as anodes. First we calculate the energy barrier of Li diffusion through N and B doped pristine graphene. N doped pristine graphene has a positive adsorption energy (0.75 eV) denoting the weak bonding between graphene and Li. In this system, nitrogen accumulates extra charge from the carbon atoms due to its higher electro-negativity, as shown in Fig. 3(a) and (b). Upon Li adsorption, it prefers to lie in the region where it can easily donate charge to carbon atoms *i.e.*, away from the N as it has excess charge. Li relaxes to a position which is 1.78 Å above the plane of graphene. The energy barrier for Li to diffuse through was found to be very high at 16.80 eV, making this system a poor choice for Li diffusion.

The adsorption energy of Li on B doped graphene is −1.40 eV, indicating the optimal stability of the structure. Boron transfers all its charge to carbon atoms due to its electro-positive nature. Li also donates one electron to the host carbon matrix. This is further confirmed by the isosurfaces of the total charge, which shows no charge at the B and Li sites, Fig. 3(c) and (d). The energy barrier of 8.69 eV for Li diffusion through this sheet is lower than that of undoped pristine graphene. Hence, B turns out to be a better choice for storage of Li compared to N, though the barrier is not low enough to give faster Li diffusion.

In order to understand the effect of doping on the electronic structure of the host graphitic material, we calculated the density of states (DOS) for pristine, N and B doped graphene in the absence and presence of Li, as shown in Fig. 4. Since we considered the cluster model, DOS is finite at the Fermi level instead of the semi-metallic nature of the infinite 2D graphene sheet. The peak observed above the Fermi level in the partial DOS (PDOS) of Li-2s clearly shows that Li is ionized. In the case of N doping, the PDOS indicates that the states just below the Fermi level are originating from the N-2p, which are completely filled. Therefore, N doped pristine graphene will not withdraw more electrons from Li, which leads to the high barrier compared to pristine graphene. The Li-2s peak lies above the Fermi level for both the pristine and N doped graphene at nearly the same position. This indicates the similar interaction of Li in these two systems leading to almost the same positive adsorption energy. On the other hand, the B-doped graphene Li-2s peak lies far above the Fermi level and hence exhibits the strongest adsorption energy. Furthermore, the PDOS for B-2p

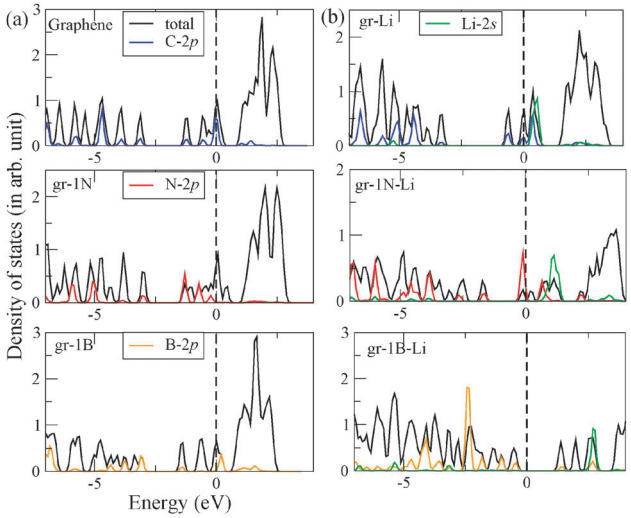

Fig. 4 Density of states for pristine, B and N doped graphene in the (a) absence and (b) presence of Li.

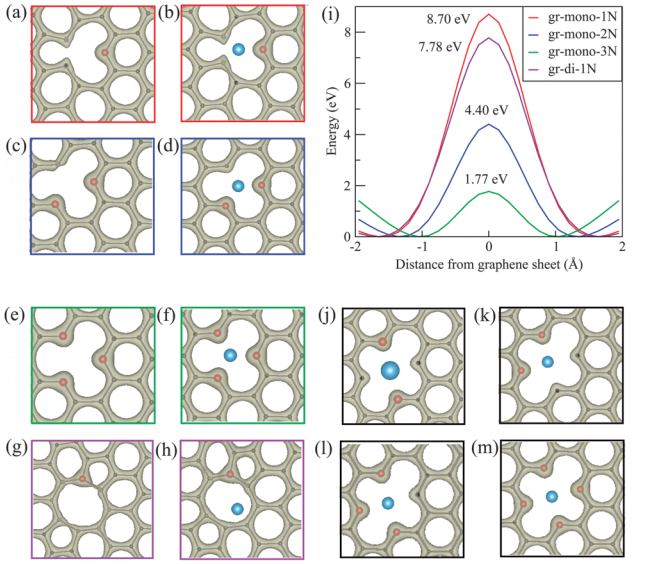

Fig. 5 Isosurfaces of total electronic charge density for graphene: monovacancy doped by one N (a) without and (b) with Li, by two N (c) without and (d) with Li, and by three N (e) without and (f) with Li; divacancy doped by one N (g) without and (h) with Li, (i) corresponding energy barriers, divacancy doped by (j) two N (type 1), (k) two N (type 2), (l) three N and (m) four N.

denotes that there are empty states above the Fermi level, which helps to withdraw electrons from Li and hence causes a lower energy barrier.

Next, we estimate the diffusion barriers through N and B doped defected graphene. Nitrogen and boron have been doped in graphene with mono- and divacancies. For the monovacancy case, graphene has been doped with 1, 2 and 3 nitrogen forming pyridine-type configurations,[42] as shown in Fig. 5(a), (c) and (e). A monomeric pyridine-type defect (Fig. 5(a)) gives an 8.70 eV energy barrier. This barrier is comparable to the one obtained for pristine graphene with a monovacancy. Doping with additional N (a dimerized pyridine-type defect) reduces the energy barrier by almost half to 4.40 eV. In the presence of three N (trimerized pyridine-type defect), the barrier becomes even smaller to 1.77 eV. The barrier reduces due to the removal of radicals as a function of the number of nitrogen atoms. In the case of three N, all the radicals are removed from the edge of the vacancy, which leads to a lower interaction with the Li, thereby reducing the energy barrier to a range which is favorable for faster kinetics. C–N bond lengths are between 1.33 and 1.36 Å, slightly less than that of C–C bond lengths in pristine graphene (1.42 Å). All the systems remain almost planar, with N protruding out of the plane of the sheet due to the attraction from the Li ion. Adsorption energies of Li for one, two and three N doped graphene with monovacancy sheets are −1.69 eV, −1.64 eV and −3.28 eV, respectively. Though graphene with a trimerized pyridine-type defect has the lowest barrier for Li, its strong adsorption energy caused by the coulombic attraction with three N will make the de-lithiation process very difficult.

Next, we study the effect of N doping in the graphene with the divacancy. Once again, the area in the vicinity of the divacancy was doped by one, two, three and four nitrogens, respectively as illustrated in Fig. 5(e)–(h) and (j)–(m). Li prefers to bind almost in the plane of graphene for all the N doped systems except one N. The single N doped configuration has the lowest adsorption energy. The configurations with two, three and four N atoms have higher adsorption energies (−2.64 to −3.54 eV). Graphene with a divacancy doped by one N, forms a pyrrolic type-defect. The relaxed structure with Li buckles significantly due to the attraction between the Li ion and the lone pair of N and gives a comparatively larger barrier of 7.78 eV. Bond lengths between C and N lie in the range of 1.43 to 1.48 Å, slightly greater than the C–C bond length in pristine graphene. There are two symmetrically inequivalent configurations for two N doped graphenes. Li prefers to lie slightly above the plane of graphene for both types of configuration, as illustrated in Table 2. Furthermore, in the three and four N doped systems, the Li lies almost in the plane of the sheet. The coulombic attraction between the negatively charged nitrogen and the positively charged Li ion causes the strong adsorption energy in these cases. For two, three and four N doping, C–N bond lengths shrink and lie between 1.34 and 1.36 Å. Li prefers to stay almost in the plane of the sheet as well as at the centre of the vacancy, and there are no local minima for Li above the plane of the sheet. Therefore, there is a large amount of energy (equivalent to adsorption energies) required to remove the Li. The adsorption energies are slightly higher and it would be difficult to remove the Li once it gets trapped in the vicinity of the N doped divacancy.

Furthermore, we study the effect of boron doping on the Li diffusion barrier through the graphene with mono and divacancy. Boron doping of graphene with monovacancy, as shown in Fig. 6, leads to a high energy barrier of (i) 31.67 eV for one, (ii) 15.43 eV for two and (iii) 13.33 eV for three borons, which makes it almost impossible for Li to diffuse. Repulsion between electropositive B and positively charged Li leads to comparatively less adsorption energies of (i) −2.30 eV, (ii) −0.36 eV and (iii) −1.20 eV for one, two, and three B doped

Table 2 Adsorption energy (E_{ad}) of Li, distance of Li from the graphene sheet (d) and energy barrier (E_b) for the systems studied are listed below:

System	E_{ad} (eV)	d (Å)	E_b (eV)
Pristine graphene	0.71	1.72	10.02
Gr-mono	−2.03	2.00	8.18
Gr-di	−0.55	1.40	1.34
Gr-Stone–Wales	−0.65	2.07	6.23
Gr-1N	0.75	1.79	16.80
Gr-mono-1N	−1.69	1.77	8.70
Gr-mono-2N	−1.64	1.57	4.40
Gr-mono-3N	−3.28	1.50	1.77
Gr-di-1N	−1.30	1.72	7.78
Gr-di-2N(type 1)	−3.06	0.42	—
Gr-di-2N(type 2)	−2.64	0.74	—
Gr-di-3N	−3.31	0.30	—
Gr-di-4N	−3.54	0.11	—
Gr-1B	−1.40	1.69	8.69
Gr-mono-1B	−2.30	1.72	31.67
Gr-mono-2B	−0.36	1.89	15.43
Gr-mono-3B	−1.20	1.78	13.33
Gr-di-1B	−1.25	1.35	1.68
Gr-di-2B(type 1)	−1.49	1.29	1.67
Gr-di-2B(type 2)	−1.14	1.26	1.54
Gr-di-3B	−1.59	1.29	1.74
Gr-di-4B	−1.47	1.26	1.78

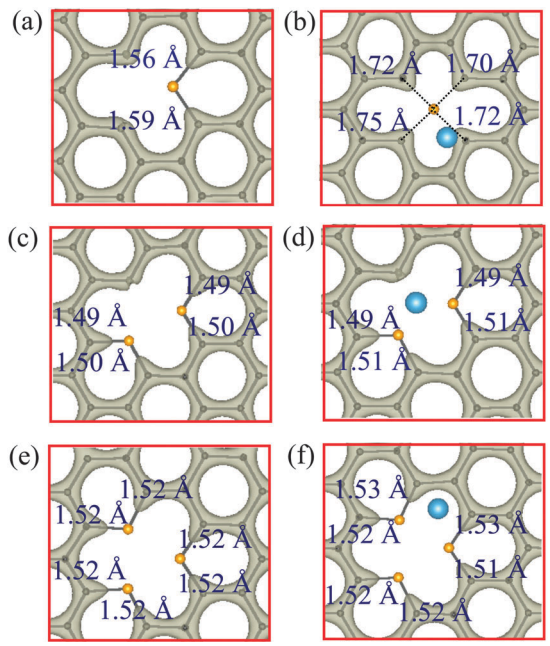

Fig. 6 Isosurfaces of total electronic charge density for graphene with a monovacancy doped by: one B (a) without and (b) with Li, two B (c) without and (d) with Li, three B (e) without and (f) with Li.

graphene with a monovacancy. After B doping, the C–B bond elongates compared to the C–C bond length in pristine graphene.[43] For the single B doped case, bond lengths between B and the two nearest C atoms are 1.59 and 1.56 Å (see Fig. 6(a)). In the presence of Li, B shifts to the center of the defect with a distance of 1.70 to 1.75 Å from the nearest four C atoms and Li lies 1.72 Å above the plane of the graphene. The graphene sheet buckles significantly and Li moves far from the center of the defect as a result of the repulsion between one B atom and the Li ion. In the case of monovacancy graphene doped with two B, the repulsion between the two B atoms does not allow the C–B bond length to increase. The resultant repulsion of the two electropositive B atoms from the Li ion maintains the planar structure of the system, providing the lowest adsorption energy among all the configurations. Li relaxes at 1.89 Å above the center of the defect. The C–B bond length increases slightly in the case of three B doping. In this case, Li prefers to lie far from the B atoms, 1.78 Å above the graphene plane. The C–B bond lengths for two bonds neighboring the Li ion elongates compared with the other C–B bonds. Here also, the planar structure of the doped graphene sheet is retained due to the resultant B–Li repulsion. Overall, the adsorption energies are in the optimal range, however a high barrier makes these systems an unsuitable candidate for an anode material.

Next, graphene with divacancy was doped by one, two, three and four boron atoms. The energy barrier remains significantly low and lies in the range of 1.54 to 1.78 eV, for all the different types of configurations and doping concentrations. This is commensurate with the adsorption energies, which are also very low, from −1.14 eV to −1.59 eV for all the cases due to the repulsion between electropositive B and the positively charged Li. In Fig. 7, boron doped structures with a divacancy and the corresponding energy barrier are shown. Li prefers to stay at the center of the defect for one, two and four B doped divacancy graphenes and slightly off from the center for the three B doped case. There is no significant buckling for all the systems. The divacancy forms an octagon surrounded by two pentagons and hexagons in all the configurations and hence provides a much larger space for Li to diffuse easily. The repulsion between B and the Li ion provides the appropriate conditions to keep both the adsorption energy and the energy barrier at a moderate value. The trend of getting almost the same adsorption energy and same energy barrier can be explained from the density of states as shown in Fig. S2 (ESI†). The peak in the conduction band in the partial DOS of Li remains almost in the same position for all the B doped divacancy cases, demonstrating similar interaction between the Li and B. Therefore, B doped

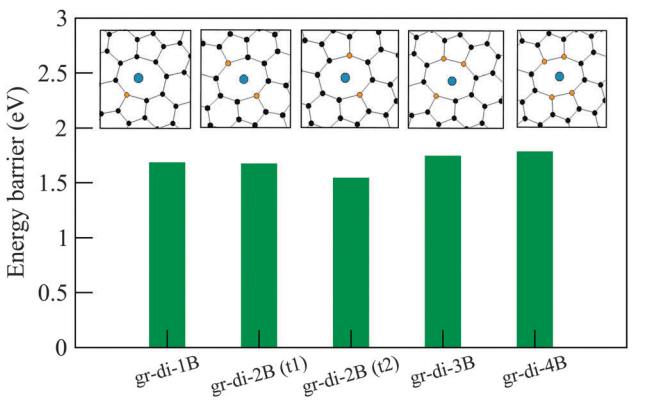

Fig. 7 Relaxed structures and corresponding energy barriers for B-doped graphene with a divacancy.

graphene with a divacancy can be very promising for both anode materials and artificial SEI to protect the anode.

4 Conclusions

In summary, we comprehensively study the possibility of using doped defected-graphene as a potential anode material. The energy barrier for Li to diffuse through the pristine graphene is very high. The presence of defects such as Stone–Wales, mono- and divacancies reduces the barrier significantly. Among these, adding a divacancy has the lowest barrier of 1.34 eV, which would lead to good kinetics at ambient conditions. The doping of pristine graphene with B improves the binding energies, however the barriers remain very high. The effect of B and N doping of defected graphene on the energy barriers have been studied. The Li diffusion barrier through the N doped graphene with a monovacancy decreases as a function of the number of N atoms. Out of all the N doped monovacancy cases, the three N doped system gives the lowest barrier. In the case of the N doped divacancy, Li prefers to lie in the plane of the graphene sheet with strong adsorption energy except for the one N doped case. Doping a graphene with a monovacancy by B leads to a high diffusion barrier. On the other hand, for a divacancy, both energy barriers and adsorption energies are significantly lower for all the configurations. Boron doped defected graphene turns out to be most promising candidate for anode materials in Li ion batteries. Our results reveal the problems and advantages of pristine, doped, and doped defected graphene, which would help to model a suitable anode material or coating material as an artificial SEI in a Li ion battery.

Acknowledgements

D.D. and A.K.S. thankfully acknowledge the financial support from the Korea Institute of Science and Technology (Grant No. 2E23920), S.K. and K.-R.L. were supported by the Industrial Strategic Technology Development Program (Grant No. 10041589) funded by the Ministry of Knowledge Economy (MKE, Korea). The authors thankfully acknowledge Dr Rahul P. Hardikar for useful discussions. We thankfully acknowledge the Materials Research Centre and Supercomputer Education and Research Centre, Indian Institute of Science for computing facilities.

References

1 K. Kang, Y. S. Meng, J. Brger, C. P. Grey and G. Ceder, *Science*, 2006, **311**, 977–980.
2 B. Kang and G. Ceder, *Nature*, 2009, **458**, 190–193.
3 M. Armand, S. Grugeon, H. Vezin, S. Laruelle, P. Ribiere, P. Poizot and J.-M. Tarascon, *Nat. Mater.*, 2009, **8**, 120–125.
4 M. Morcrette, P. Rozier, L. Dupont, E. Mugnier, L. Sannier, J. Galy and J.-M. Tarascon, *Nat. Mater.*, 2003, **2**, 755–761.
5 K. Zaghib, A. Mauger, H. Groult, J. B. Goodenough and C. M. Julien, *Materials*, 2013, **6**, 1028–1049.
6 L. Su, Y. Jing and Z. Zhou, *Nanoscale*, 2011, **3**, 3967–3983.
7 J.-M. Tarascon and M. Armand, *Nature*, 2001, **414**, 359–367.
8 Y. Nishi, *J. Power Sources*, 2001, **100**, 101–106.
9 T. D. Hatchard and J. R. Dahn, *J. Electrochem. Soc.*, 2004, **151**, A838–A842.
10 J. P. Maranchi, A. F. Hepp and P. N. Kumta, *Electrochem. Solid-State Lett.*, 2003, **6**, A198–A201.
11 L. Y. Beaulieu, K. W. Eberman, R. L. Turner, L. J. Krause and J. R. Dahn, *Electrochem. Solid-State Lett.*, 2001, **4**, A137–A140.
12 B. Wang, X. Li, X. Zhang, B. Luo, M. Jin, M. Liang, S. A. Dayeh, S. T. Picraux and L. Zhi, *ACS Nano*, 2013, **7**, 1437–1445.
13 A. A. Arie, J. O. Song and J. K. Lee, *Mater. Chem. Phys.*, 2009, **113**, 249–254.
14 S. Yang, Y. Gong, Z. Liu, L. Zhan, D. P. Hashim, L. Ma, R. Vajtai and P. M. Ajayan, *Nano Lett.*, 2013, **13**, 1596–1601.
15 Z.-S. Wu, W. Ren, L. Xu, F. Li and H.-M. Cheng, *ACS Nano*, 2011, **5**, 5463–5471.
16 D. Zhou, Y. Cui and B. Han, *Chin. Sci. Bull.*, 2012, **57**, 2983–2994.
17 E. Yoo, J. Kim, E. Hosono, H.-s. Zhou, T. Kudo and I. Honma, *Nano Lett.*, 2008, **8**, 2277–2282.
18 A. S. Arico, P. Bruce, B. Scrosati, J.-M. Tarascon and W. van Schalkwijk, *Nat. Mater.*, 2005, **4**, 366–377.
19 G. Kresse and J. Hafner, *Phys. Rev. B: Condens. Matter*, 1993, **47**, 558–561.
20 G. Kresse and D. Joubert, *Phys. Rev. B: Condens. Matter Mater. Phys.*, 1999, **59**, 1758–1775.
21 P. E. Blöchl, *Phys. Rev. B: Condens. Matter*, 1994, **50**, 17953–17979.
22 J. P. Perdew, K. Burke and M. Ernzerhof, *Phys. Rev. Lett.*, 1996, **77**, 3865–3868.
23 G. Kresse and J. Furthmller, *Comput. Mater. Sci.*, 1996, **6**, 15–50.
24 G. Makov and M. C. Payne, *Phys. Rev. B: Condens. Matter*, 1995, **51**, 4014–4022.
25 G. Henkelman, B. P. Uberuaga and H. Jonsson, *J. Chem. Phys.*, 2000, **113**, 9901–9904.
26 G. Mills and H. Jónsson, *Phys. Rev. Lett.*, 1994, **72**, 1124–1127.
27 F. Yao, F. Gne, H. Q. Ta, S. M. Lee, S. J. Chae, K. Y. Sheem, C. S. Cojocaru, S. S. Xie and Y. H. Lee, *J. Am. Chem. Soc.*, 2012, **134**, 8646–8654.
28 X. Zhao, C. M. Hayner, M. C. Kung and H. H. Kung, *ACS Nano*, 2011, **5**, 8739–8749.
29 A. Stone and D. Wales, *Chem. Phys. Lett.*, 1986, **128**, 501–503.
30 K. Suenaga, H. Wakabayashi, M. Koshino, Y. Sato, K. Urita and S. Iijima, *Nat. Nanotechnol.*, 2007, **2**, 358–360.
31 H. Wu, G. Chan, J. W. Choi, I. Ryu, Y. Yao, M. T. McDowell, S. W. Lee, A. Jackson, Y. Yang, L. Hu and Y. Cui, *Nat. Nanotechnol.*, 2012, **7**, 310–315.
32 A. L. M. Reddy, A. Srivastava, S. R. Gowda, H. Gullapalli, M. Dubey and P. M. Ajayan, *ACS Nano*, 2010, **4**, 6337–6342.
33 F. Banhart, J. Kotakoski and A. V. Krasheninnikov, *ACS Nano*, 2011, **5**, 26–41.
34 L. Qu, Y. Liu, J.-B. Baek and L. Dai, *ACS Nano*, 2010, **4**, 1321–1326.
35 G. Wu, N. H. Mack, W. Gao, S. Ma, R. Zhong, J. Han, J. K. Baldwin and P. Zelenay, *ACS Nano*, 2012, **6**, 9764–9776.

36 Y. Li, Z. Zhou, P. Shen and Z. Chen, *ACS Nano*, 2009, **3**, 1952–1958.
37 Y. F. Li, Z. Zhou and L. B. Wang, *J. Chem. Phys.*, 2008, **129**, 104703.
38 Z. Zhou, J. Zhao, X. Gao, Z. Chen, J. Yan, P. von Ragu Schleyer and M. Morinaga, *Chem. Mater.*, 2005, **17**, 992–1000.
39 J. Zhao, B. Wen, Z. Zhou, Z. Chen and P. v. R. Schleyer, *Chem. Phys. Lett.*, 2005, **415**, 323–326.
40 C. Ma, X. Shao and D. Cao, *J. Mater. Chem.*, 2012, **22**, 8911–8915.
41 Y. Liu, V. I. Artyukhov, M. Liu, A. R. Harutyunyan and B. I. Yakobson, *J. Phys. Chem. Lett.*, 2013, **4**, 1737–1742.
42 Y. Fujimoto and S. Saito, *Phys. Rev. B: Condens. Matter Mater. Phys.*, 2011, **84**, 245446.
43 L. S. Panchakarla, K. S. Subrahmanyam, S. K. Saha, A. Govindaraj, H. R. Krishnamurthy, U. V. Waghmare and C. N. R. Rao, *Adv. Mater.*, 2009, **21**, 4726–4730.

